Journal of Alloys and Compounds 509 (2011) L199–L202

Contents lists available at ScienceDirect

Journal of Alloys and Compounds

journal homepage: www.elsevier.com/locate/jallcom

Letter

Preparation and its luminescent properties of $AlPO_4$:Eu^{3+} phosphor for w-LED applications

Yu-feng Liu[a,*], Zhi-ping Yang[a], Quan-mao Yu[b]

[a] College of Physics Science and Technology, Hebei University, Baoding 071002, PR China
[b] Institute of Functional Materials, Jiangxi University of Finance & Economics, Nanchang 330013, PR China

ARTICLE INFO

Article history:
Received 6 October 2010
Received in revised form 5 March 2011
Accepted 8 March 2011
Available online 16 March 2011

Keywords:
Phosphors
Solid state reactions
Optical properties
Luminescence

ABSTRACT

Orange-reddish-emitting phosphor $AlPO_4$:Eu^{3+} were fabricated by solid-state reactions at high temperature. X-ray diffraction analysis revealed that $AlPO_4$ doped with 3 mol% of Eu^{3+} ($AlPO_4$:$0.03Eu^{3+}$) was pure orthorhombic phase. The photoluminescence study shows that the intensity of magnetic dipole transition ($^5D_0 \to {}^7F_1$) at 594 nm dominates over that of electric dipole transition ($^5D_0 \to {}^7F_2$) at 613 nm. The optimum concentration of Eu^{3+} for the highest luminescence is found to be 3 mol%. The PL excitation spectrum is composed of CTB of Eu–O and excitation lines of Eu^{3+} ions. The strongest excitation lines appeared at 392 nm. The color coordinates, quantum yield and lifetime for $AlPO_4$:$0.03Eu^{3+}$ were measured. All the spectrum features indicate that $AlPO_4$:Eu^{3+} might be a promising phosphor for display devices or w-LEDs.

1. Introduction

The most popular approach to fabricating white-light emitting diodes (w-LEDs) is by coating a yellow emitting phosphor on a blue emitting InGaN LED. Yttrium aluminum garnet doped with cerium (YAG:Ce) is commonly used as the yellow phosphor for this purpose. However, w-LEDs fabricated in this way give bi-chromatic white light with poor color quality (CRI ~ 70) due to lack of red component [1,2]. One of the most promising approaches to generate white light in w-LEDs is to use a LED emitting near-UV light (UV-LED, 360–400 nm) coated with blue, green and red tri-color phosphors. This approach yields a more balanced white spectrum than the traditional devices of blue emitter + yellow phosphor and is easier to be controlled than the devices in which the white light is generated by the combination of individual red, green and blue LEDs [3–5]. Many researches have been conducted in order to develop new red phosphors suitable for UV-LED excitations [6–9]. However, up to now, satisfied red phosphors for the w-LED applications are not available.

Phosphates are a type of promising host materials for their easy-synthesis, low-cost and chemical/thermal-stabilities over a wide range of temperatures (400–800 °C) [10]. $AlPO_4$ is a well-known artificial material as molecular sieve [11]. Long and co-workers first reported the partial substitution of Al^{3+} by Eu^{3+} in a small-pore (eight-membered ring channel) microporous aluminophosphate $AlPO_4$-CJ_2 [12]. Yan et al. reported the substitution of rare earth (RE) elements (Eu, Ce, Tb) on the large-pore aluminophosphate and mesoporous aluminophosphate [13]. These materials have potential applications in catalysis, phosphors, lasers, optical amplifiers, filters, and optical memories. However, to the best of our knowledge, few attentions have been paid to the luminescent properties of RE doped $AlPO_4$ as a luminescent material [14,15]. In this letter, we first report the synthesis and characterization of orange-reddish-emitting $AlPO_4$:Eu^{3+} powders. Our work shows that $AlPO_4$:Eu^{3+} has a strong absorption peak at $\lambda = 392$ nm and gives orange-reddish emissions, which offers an excellent possibility for w-LED applications.

2. Experimental

Microcrystalline powder of $AlPO_4$:Eu^{3+} with Eu^{3+} concentration 3 mol% ($AlPO_4$:$0.03Eu^{3+}$) was prepared by solid-state reactions. Raw materials used in the experiment were Al_2O_3(≥99.9%), $NH_4H_2PO_4$ (≥99.9%) and Eu_2O_3 (99.99%). The raw materials with stoichiometrical ratio were weighed and mixed in mortar sufficiently. In order to obtain the target compound with pure phase, two firing steps were necessary. The mixture was firstly heated at 500 °C for 2 h in a covered alumina crucible, then reground thoroughly after cooled down to the room temperature. The second firing was conducted at 1200 °C for 48 h. The same method was followed for the preparation of all the different concentrations of Eu^{3+}-doped $AlPO_4$ particles by taking the required stoichiometric amounts of the sources.

The powder sample was characterized by X-ray diffraction (XRD) in a Bruker AXS D8 advanced automatic diffractometer (Bruker Co., Germany) with Cu $K_{\alpha 1}$ radiation ($\lambda = 1.5405$ Å). Photoluminescence (PL) excitation and emissions spectra were collected in a fluorescence spectrophotometer (Hitachi FL-4600). The chromaticity data were taken by using the PMS-50 spectra analysis system. Spectra for the quantum yield (η) measurement were collected using an integrated sphere. Powder samples were mixed with appropriate methanol, spread over a quartz plate, dried at ambient atmosphere, and mounted inside the sample chamber of the integrated sphere. Lifetime measurement for Eu^{3+} transitions was carried out using μs flash lamp

---

* Corresponding author. Tel.: +86 0312 5079423; fax: +86 0312 5011174.
E-mail address: liuyufeng4@126.com (Y.-f. Liu).

0925-8388/$ – see front matter © 2011 Elsevier B.V. All rights reserved.
doi:10.1016/j.jallcom.2011.03.064

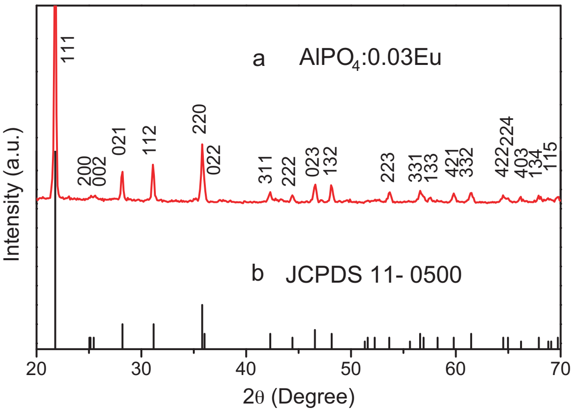

Fig. 1. XRD patterns of $AlPO_4$:0.03Eu^{3+} phosphor (a) and JCPDS data (b, No. 11-0500).

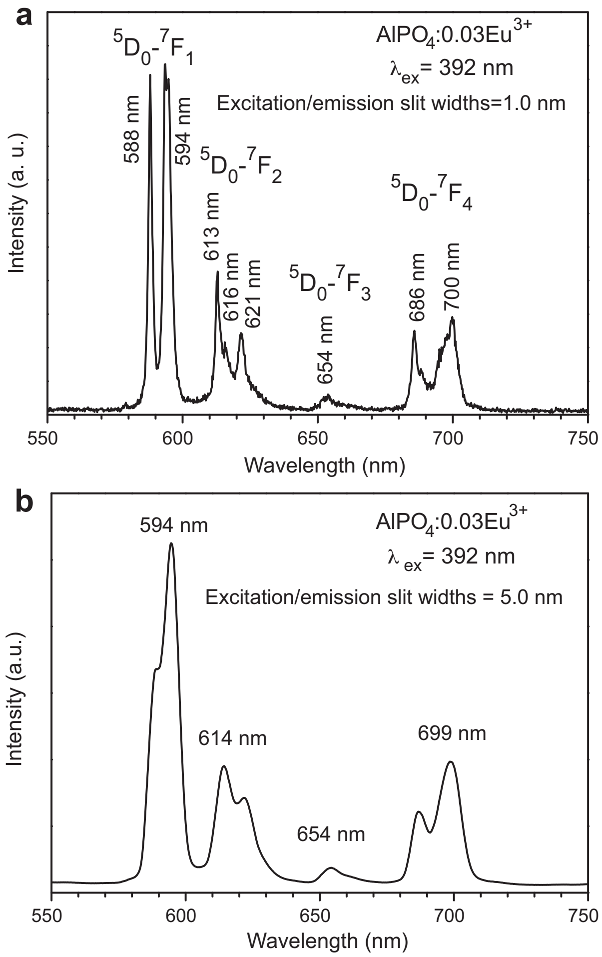

Fig. 2. PL emission spectra of $AlPO_4$:0.03Eu^{3+} under the excitation of 392 nm (λ_{ex} = 392 nm) ((a) excitation/emission slit widths = 1.0 nm and (b) excitation/emission slit widths = 5.0 nm).

attached to Edinburgh Instruments (model FLS920). All the measurements were conducted at room temperature.

3. Results and discussion

$AlPO_4$ has an orthorhombic crystal structure with a space group of $C222_1$ (No. 20) and lattice parameters values a = 7.082 Å, b 7.098 Å, c 6.993 Å, and V = 351.52 (Å^3), Z = 4 [16]. Fig. 1 represents the XRD patterns of $AlPO_4$:0.03Eu^{3+} and JCPDS data (No. 11-0500). The comparison of measured powder XRD patterns of $AlPO_4$:0.03Eu^{3+} with that of JCPDS data (No. 11-0500) indicates that the as-synthesized products were well crystallized with the $AlPO_4$ structure and no (detectable) additional phases (such as Eu_2O_3, $EuPO_4$) or other crystalline impurity phase present. The concentration of Eu^{3+} is 3 atom percent in the as-synthesized $AlPO_4$ materials. The substitution of Al^{3+} by the Eu^{3+} ion is expected to be random in the framework. Therefore, no obvious differences in the XRD peaks positions are noted between the as-synthesized material and the JCPDS data (No. 11-0500). To further rule out the existence of the $EuPO_4$ in the final products possibility, additional experiment was performed by synthesizing the $EuPO_4$ for spectral comparison. The fluorescent pattern of the $EuPO_4$ (not shown) is very different from that of the $AlPO_4$:Eu^{3+}. This difference along with XRD results indicates that no $EuPO_4$ exists in the final product $AlPO_4$:Eu^{3+}.

Fig. 2a shows the PL emission spectrum of $AlPO_4$:0.03Eu^{3+} obtained under the excitation of λ = 392 nm. The strongest doublet peak located at 588 nm and 594 nm contribute the orange-reddish emission, which are mainly from the $^5D_0 \rightarrow {}^7F_1$ magnetic dipole transitions of Eu^{3+} ions and the weak red emissions peaked at 613 nm and 621 nm are due to the hypersensitive $^5D_0 \rightarrow {}^7F_2$ electric dipole transition.

The emission spectrum consist of sharp lines as expected is the transitions between f–f levels of Eu^{3+} ($^5D_0 \rightarrow {}^7F_{1,2}$). The emission spectrum of Eu^{3+} is very sensitive to the local environment. The intensity of the electric dipole $^5D_0 \rightarrow {}^7F_2$ transition is significantly affected by the degree of symmetry environment around Eu^{3+} ions. Conversely, the $^5D_0 \rightarrow {}^7F_1$ emission is allowed by the magnetic dipole consideration and is therefore, relatively insensitive to the local symmetry. If more Eu^{3+} ions occupy the inversion site, the emission intensity from the $^5D_0 \rightarrow {}^7F_1$ transition will be enhanced and the phosphors will primarily exhibit orange-red luminescence [17]. In $AlPO_4$:0.03Eu^{3+}, the emissions of magnetic dipole $^5D_0 \rightarrow {}^7F_1$ transition at 588 nm and 594 nm are relatively more intense than that of the electronic dipole $^5D_0 \rightarrow {}^7F_2$ transition at about 613 nm and 621 nm, it shows that the Eu^{3+} occupied more inversion symmetry sites in $AlPO_4$ [17].

The symmetry around the Eu^{3+} ions in the $AlPO_4$ environment also can be understood using a ratio of intensities (A_{21}) of electric dipole transition to magnetic dipole transition (called asymmetric ratio A_{21}) which is defined as [18]:

$$A_{21} = \frac{\int I_2 d\lambda}{\int I_1 d\lambda} \tag{1}$$

where I_1 and I_2 represent the respective integrated intensity of $^5D_0 \rightarrow {}^7F_1$ and $^5D_0 \rightarrow {}^7F_2$ transitions of Eu^{3+}, respectively. In all the samples the asymmetric ratio values are found to be less than unity indicating the occupation of more Eu^{3+} ions at inversion symmetry site. Similar observation was reported on Eu^{3+} doped $LnPO_4$ (Ln = Y, La, Gd) materials irrespective of crystal structure (tetragonal, hexagonal and monoclinic phases) [18,19].

According to the relationship of the group theory and Eu^{3+} emission spectrum, if the Eu^{3+} ions occupy the C_i, C_{2h} or D_{2h} symmetry site, the emission of $^5D_0 \rightarrow {}^7F_1$ will present three sharp lines; If the Eu^{3+} ions occupy the C_{4h}, D_{4h}, D_{3d}, S_6, C_{6h} or D_{6h} symmetry site, the emission of $^5D_0 \rightarrow {}^7F_1$ will present two sharp lines; If the Eu^{3+} ions occupy the T_h or O_h symmetry site, the emission of $^5D_0 \rightarrow {}^7F_1$ will present one sharp line. On the other hand, splitting for Eu^{3+} emissions from $^5D_0 \rightarrow {}^7F_{1,2}$ depends on the following: (I) intensity of the exciting source, (II) excitation/emission slit widths, and (III) crystallinity. Increase of both (I) and (III) and decrease of (II) will split $^5D_0 \rightarrow {}^7F_{1,2}$ transition [17]. In the present study, the Eu^{3+} substituted for Al^{3+} ion at random and occupied C_{4h} site in the framework of $AlPO_4$. Additionally, we used high intensity of excitation source (450 W xenon lamps) and small

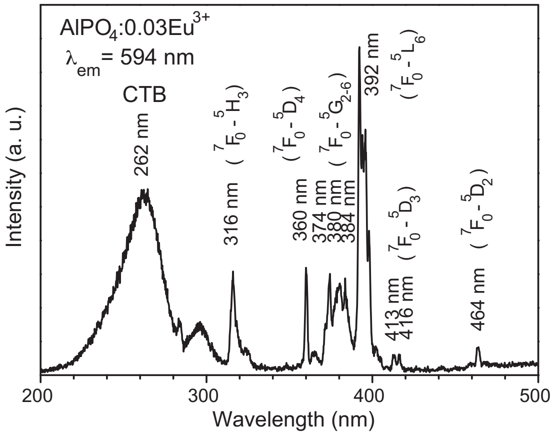

Fig. 3. PL excitation spectrum of $AlPO_4$:$0.03Eu^{3+}$ monitoring emission at 594 nm (λ_{em} = 594 nm).

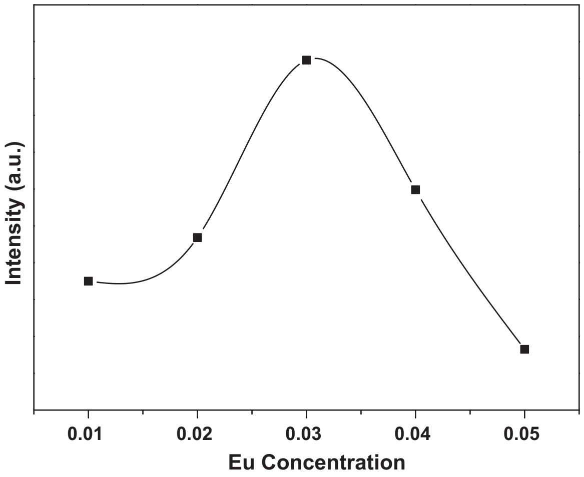

Fig. 4. Concentration dependence of relative emission intensity for $AlPO_4$:Eu^{3+}.

excitation/emission slit widths (1.0 nm), therefore, splitting of Eu^{3+} emissions from $^5D_0 \rightarrow {}^7F_1$ could be clearly observed. If increase the excitation/emission slit widths (5.0 nm), as shown in Fig. 2b, the splitting of Eu^{3+} emissions from $^5D_0 \rightarrow {}^7F_{1,2}$ could not be clearly observed. However, there are humps around 594 and 614 nm near main peaks of $^5D_0$–$^7F_{1,2}$. This is a sign of splitting [17].

Fig. 3 shows the PL excitation spectrum of $AlPO_4$:$0.03Eu^{3+}$ by monitoring emission at 594 nm. The broad peak at 262 nm is attributed to the charge transfer band (CTB) resulting from an electron transfer from the ligand O^{2-} (2p) orbital to the empty states of the $4f^6$ configuration of Eu^{3+} (Eu^{3+}–O^{2-} transition) [17,19]. The narrow excitation lines appeared at longer wavelengths correspond to the characteristic f → f transitions of Eu^{3+}. These lines are assigned as follows: $^7F_0 \rightarrow {}^5H_3$ (316 nm), $^7F_0 \rightarrow {}^5D_4$ (360 nm), $^7F_0 \rightarrow {}^5G_{2-6}$ (374, 380 and 384 nm) and the main excitation line $^7F_0 \rightarrow {}^5L_6$ (392 nm).

Various emission intensities of $AlPO_4$:Eu^{3+} are shown in Fig. 4 plotted against the concentration of Eu^{3+}. As we can see from this figure, the highest intense peak is observed at a concentration of 0.03 and then the intensity decreases gradually owing to the energy transfer between the neighboring Eu^{3+} ions, which was corresponding to the quench of the emission of Eu^{3+} [20].

The color coordinates (x = 0.6055, y = 0.3808) of $AlPO_4$:$0.03Eu^{3+}$ in the commission international de L'Eclairage (CIE) 1931 chromaticity diagram is represented in Fig. 5, which indicate that $AlPO_4$:Eu^{3+} phosphor will be useful as orange-reddish luminescence materials.

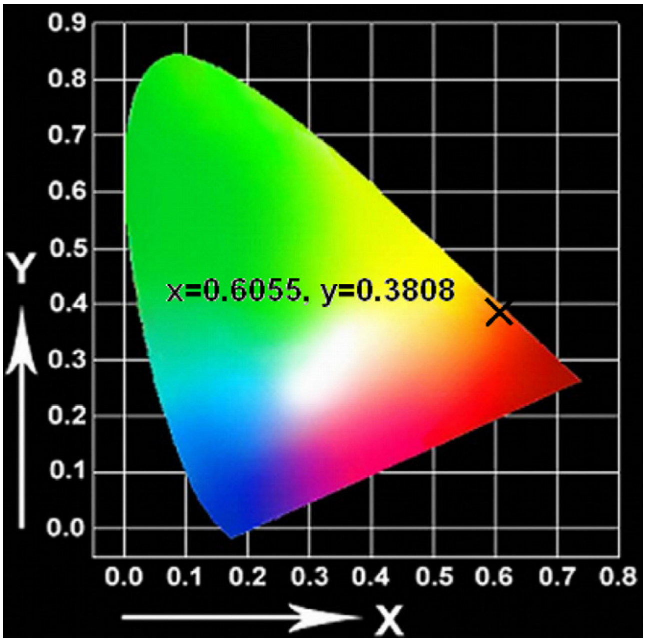

Fig. 5. Color coordinates of $AlPO_4$:$0.03Eu^{3+}$ in CIE chromaticity diagram.

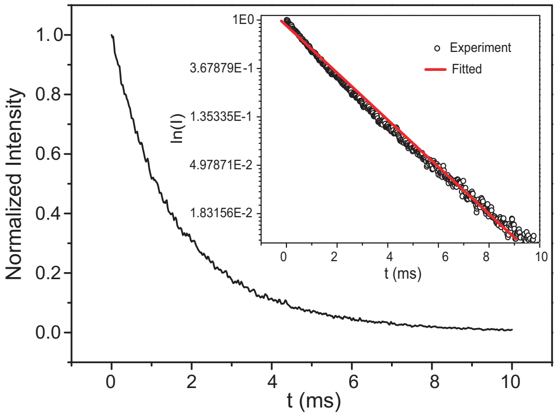

Fig. 6. Decay curves for $^5D_0 \rightarrow {}^7F_1$ of Eu^{3+} for $AlPO_4$:$0.03Eu^{3+}$ samples when excited at 392 nm. Inset shows ln(I) vs. t and data are fitted linearly.

All spectra for the quantum yield (η) measurement were collected using an integrated sphere. Quantum yield (η) is the percentage of photons emitted by a bulk sample when a given number of photons are absorbed by the samples and is given as [19]:

$$\eta = \frac{\int L_{\text{emission}}}{\int E_{\text{solvent}} - \int E_{\text{sample}}} \tag{2}$$

where L_{emission} is luminescence emission spectrum of sample, E_{solvent} is the spectrum of light used to excite the only solvent, and E_{sample} is the spectrum of light used for exciting sample. Quantum yield for $AlPO_4$:$0.03Eu^{3+}$ is found to be about 22%.

The decay curves for $^5D_0$ level of Eu^{3+} for $AlPO_4$:$0.03Eu^{3+}$ are shown in Fig. 6. Excitation wavelength was chosen at 392 nm and emission wavelength was fixed at 594 nm. For single exponential decay, it can be expressed as:

$$I = I_0 \exp\left(\frac{-t}{\tau}\right) \tag{3}$$

where I_0 and I are intensities at zero time and time t, respectively, and τ is the lifetime for transition. By taking logarithm, Eq. (3) can be written as

$$\ln(I) = \ln(I_0) - \frac{t}{\tau} \tag{4}$$

The decay data are fitted linearly and are found to follow single exponential decay for $AlPO_4$:0.03Eu^{3+} sample. Typical plot of ln(I) vs. t for $AlPO_4$:0.03Eu^{3+} is shown in Fig. 6 (inset). From the slope of plot, the life time for transition is calculated. The lifetime (τ) is found to be about 5.7 ms.

4. Conclusions

Luminescent material $AlPO_4$:Eu^{3+} were successfully fabricated by solid-state reactions at 1200 °C. The PL emission spectrum shows strong orange-reddish emission lines due to the Eu^{3+} ions. The PL excitation spectrum is composed of CTB of Eu–O and excitation lines of Eu^{3+} ions. The strongest excitation lines appeared at 392 nm. From the luminescence study the optimum concentration of luminescence is found to be 3 mol%. Lifetime study shows the single exponential behavior of the luminescence decay. The color coordinates and quantum yield for $AlPO_4$:0.03Eu^{3+} were measured.

Acknowledgments

This work was financially supported by the National Natural Science Foundation of China (Grant No. 50902042) and the Science and Technology Project of Hebei Province (Grant No. F2009000217).

References

[1] Y.H. Song, G. Jia, M. Yang, Y.J. Huang, H.P. You, H.J. Zhang, Appl. Phys. Lett. 94 (2009) 90902.
[2] T. Gessmann, E.F. Schubert, J. Appl. Phys. 95 (2004) 2203.
[3] L.Y. Zhou, J.S. Wei, J.R. Wu, F.Z. Gong, L.H. Yi, J.L. Huang, J. Alloys Compd. 476 (2009) 390.
[4] C.H. Liang, Y.C. Chang, Y.S. Chang, Appl. Phys. Lett. 93 (2008) 211902.
[5] J.S. Kima, K.T. Lima, Y.S. Jeonga, P.E. Jeon, J.C. Choi, H.L. Park, Solid State Commun. 135 (2005) 21.
[6] V.R. Bandi, M. Jayasimhadri, J. Jeong, K. Jang, H.S. Lee, S.S. Yi, J.H. Jeong, J. Phys. D: Appl. Phys. 43 (2010) 395103.
[7] H.Y. Jiao, Y.H. Wang, J.C. Zhang, J. Phys. Conf. Ser. 152 (2009) 012089.
[8] A. Xie, X.M. Yuan, F.X. Wang, Y. Shi, Z.F. Mu, J. Phys. D: Appl. Phys. 43 (2010) 055101.
[9] Z.P. Ci, Y.H. Wang, J.C. Zhang, J. Phys. Conf. Ser. 152 (2009) 012091.
[10] I.M. Nagpure, K.N. Shinde, V. Kumar, O.M. Ntwaeaborwa, S.J. Dhoble, H.C. Swar, J. Alloys Compd. 492 (2010) 384.
[11] R.A. Sheldon, I.V. Babich, Y.V. Plyuto, Mendeleev Commun. Electron. Version 3 (1997) 87.
[12] L. Zhang, C.Y. Lu, Y.C. Long, Chem. Commun. 18 (2002) 2064.
[13] W.F. Yan, Z.T. Zhang, J. Xu, S.M. Mahurin, S. Dai, Stud. Surf. Sci. Catal. 156 (2005) 265.
[14] I.F. Chang, M.W. Shafer, Appl. Phys. Lett. 35 (1979) 229.
[15] A.N. Trukhin, Solid State Commun. 90 (1994) 761.
[16] JCPDS Card No. 11-0500.
[17] N. Yaiphaba, R.S. Ningthoujam, N.S. Singh, R.K. Vatsa, N.R. Singh, J. Lumin. 130 (2010) 174.
[18] G. Phaomei, R.S. Ningthoujam, W.R. Singh, N.S. Singh, M.N. Luwang, R. Tewari, R.K. Vatsa, Opt. Mater. 32 (2010) 616.
[19] N. Yaiphaba, R.S. Ningthoujam, N.S. Singh, R.K. Vatsa, N.R. Singh, S. Dhara, N.L. Misra, R. Tewari, J. Appl. Phys. 107 (2010) 034301.
[20] D.L. Dexter, J. Chem. Phys. 22 (1954) 1063.